

# Theoretical calculations for weak transitions: $2\nu\beta\beta$ , competing decays, and the gallium anomaly



# OUTLINE

- Motivation
- Case studies
  - **$^{76}\text{Ge}$** : competing  $2\nu\beta\beta$ -decays
  - **$^{48}\text{Ca}$  and  $^{96}\text{Zr}$** :  $2\nu\beta\beta$  vs.  $\beta$ -decays
  - **$^{71}\text{Ga}$** : evidence for sterile neutrinos?
- Summary
- What am I currently working on?

# MOTIVATION: WHY TO STUDY $2\nu\beta\beta$ AND $\beta$ -DECAYS?

- Allowed by the standard model, so they definitely exist.
- A lot of unmeasured decays to be discovered.
- Many interesting cases with competing decays which can be used to test nuclear structure models.
- Advances in computing power: large-scale shell-model calculations → optimizing experiments based on theoretical half-life estimates.
- Background characterization:  $2\nu\beta\beta$ -decays are background in  $0\nu\beta\beta$ -decay experiments, rare  $\beta$ -decays in various rare-event experiments.
- Interpreting results from neutrino experiments: are we missing neutrino flux?

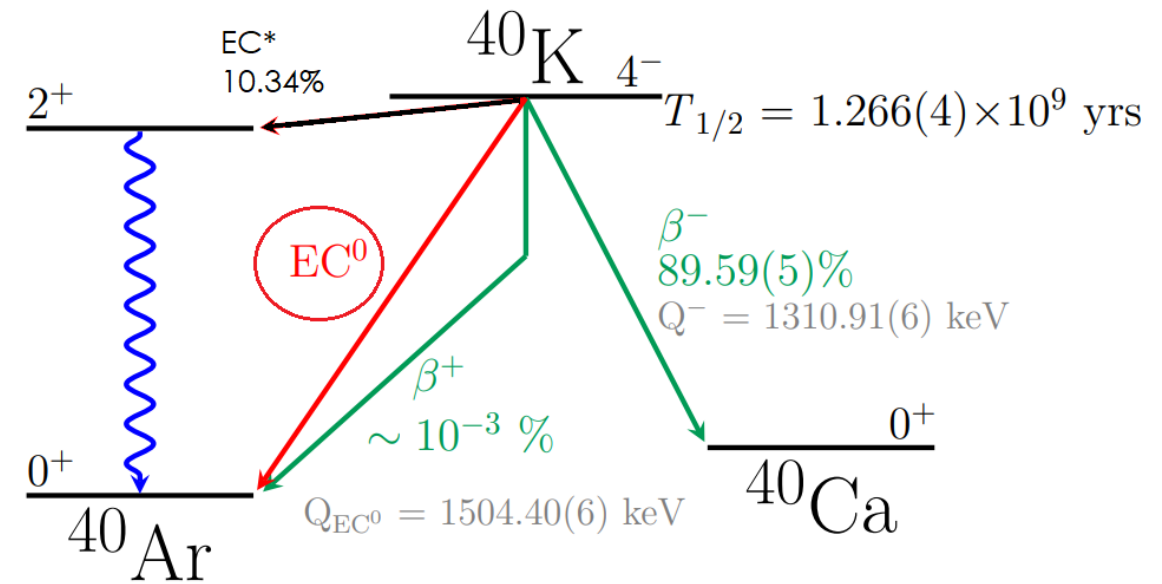
Are branching ratios, cross sections, and half-lives based on effective Hamiltonians useful?

*Uncertain uncertainties?*

*Systematic underestimation of half-lives?*

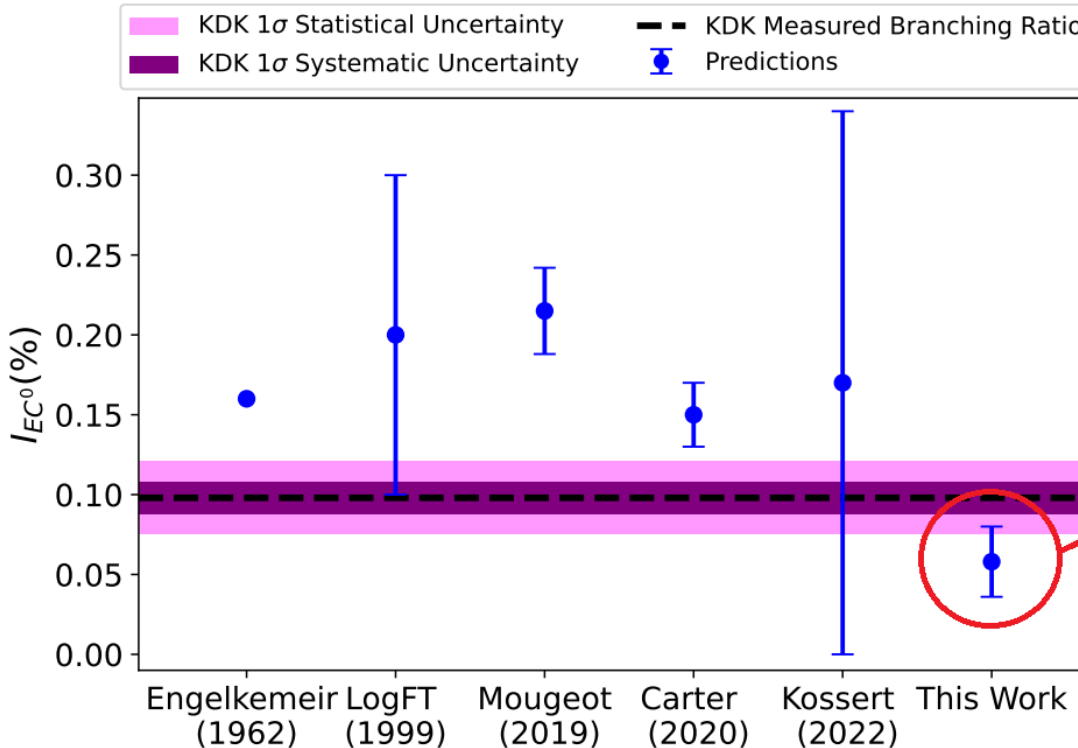
# RECENT SUCCESS STORY: $^{40}\text{K}$

- KDK Collaboration measurement of a rare  $^{40}\text{K}$  decay branch using a low-threshold x-ray detector surrounded by a tonne-scale, high-efficiency  $\gamma$ -ray tagger at Oak Ridge National Laboratory.
- Prior to conducting the experiment, the branching ratio was estimated to be  $\sim(0.06 \pm 0.03)\%$  → multiple effective Hamiltonians tested, one chosen based on its ability to produce the total half-life and EC\* branching.

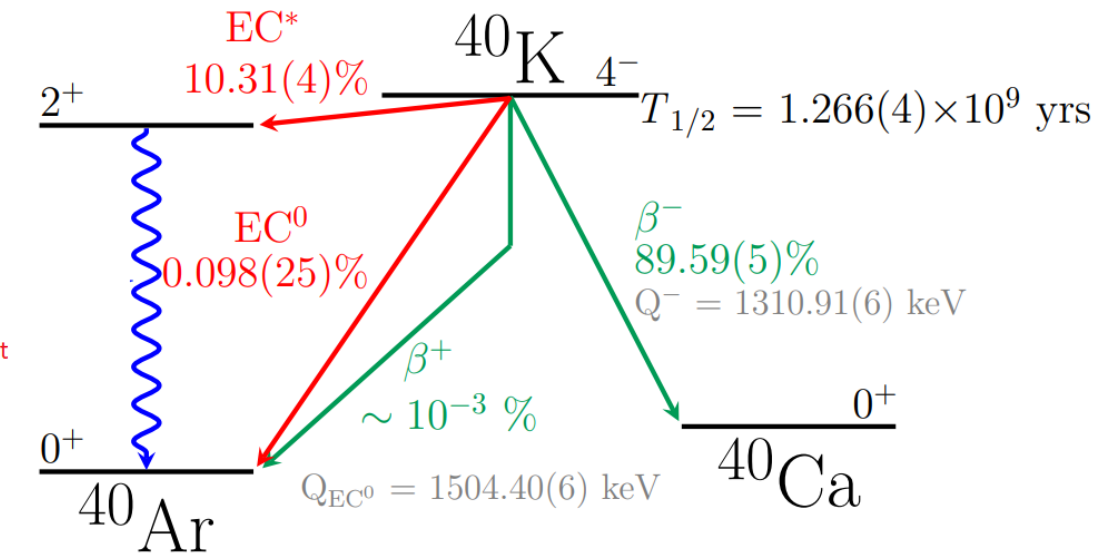


L. Hariasz *et al.* (KDK Collaboration) Phys. Rev. C **108**, 014327 – Published 31 July 2023

# RECENT SUCCESS STORY: $^{40}\text{K}$



Shell-model  
prediction using an  
effective Hamiltonian  
prior to the experiment



**Shell-model based branching ratios work!**

50% errors can be expected, but getting the magnitude right can be enough.

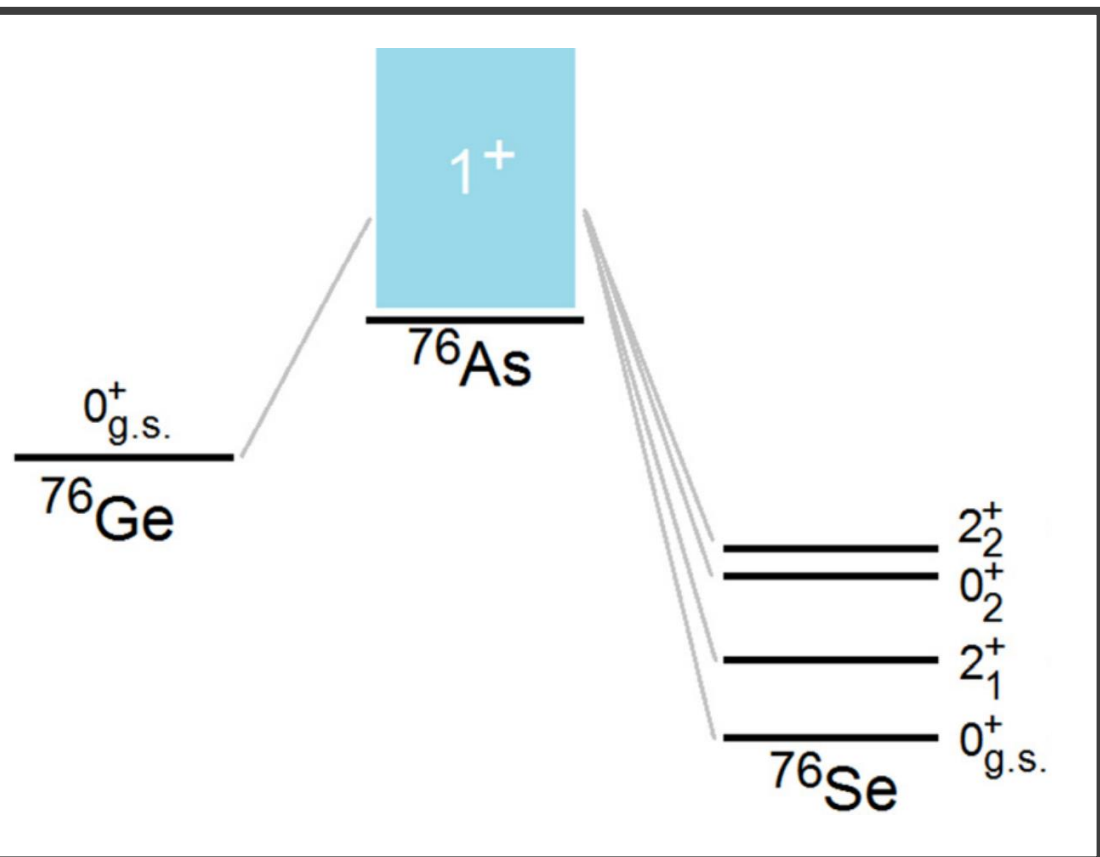
L. Hriasz *et al.* (KDK Collaboration) Phys. Rev. C **108**, 014327 – Published 31 July 2023

# $^{76}\text{Ge}$

## COMPETING $2\nu\beta\beta$ -DECAYS

Kostensalo, J., Suhonen, J., & Zuber, K. (2022). The first large-scale shell-model calculation of the two-neutrino double beta decay of  $^{76}\text{Ge}$  to the excited states in  $^{76}\text{Se}$ . *Physics Letters B*, *831*, Article 137170. <https://doi.org/10.1016/j.physletb.2022.137170>

# COMPETING $2\nu\beta\beta$



- $^{76}\text{Ge}$  has four energetically allowed  $2\nu\beta\beta$ -branches.
- The ground state is measured to high accuracy by GERDA:  $(2.022 \pm 0.018_{\text{stat}} \pm 0.038_{\text{syst}}) \times 10^{21} \text{ yr}$  [2023]
- Decays to excited states have not yet been detected. Only lower limits for half-lives exist.

# SUPPRESSION OF 2<sup>+</sup> STATES

$$M_{2\nu} = \sum_m \frac{(J^+ || \sigma\tau^- || 1_m^+)(1_m^+ || \sigma\tau^- || 0_{g.s.}^+)}{\sqrt{J+1}([\frac{1}{2}Q_{\beta\beta} + E(1_m^+) - M_i]/m_e + 1)^k}$$

Final state 0<sup>+</sup> → k = 1

Final state 2<sup>+</sup> → k = 3

**Experimental interest is on the first excited 0<sup>+</sup> state.**

# DESCRIPTION OF THE SHELL-MODEL CALCULATIONS

- Three stage calculation with a computer cluster using the effective interaction JUN45.
- 1. Calculation in the full  $0f_{5/2}$ - $1p$ - $0g_{9/2}$  model space (250 intermediate  $I^+$  states, 4.7 MeV in excitation energy)
- 2. Calculation with neutron  $0f_{5/2}$  filled (500 intermediate  $I^+$  states, include only states above the 4.7 MeV)
- 3. Calculation with neutron  $0f_{5/2}$  filled and proton  $0g_{9/2}$  empty (9999 intermediate  $I^+$  states, include all states above the excitation energy reached in step 2)

We end up with 10,266 states in total reaching 30.6 MeV.

# CUMULATIVE NME

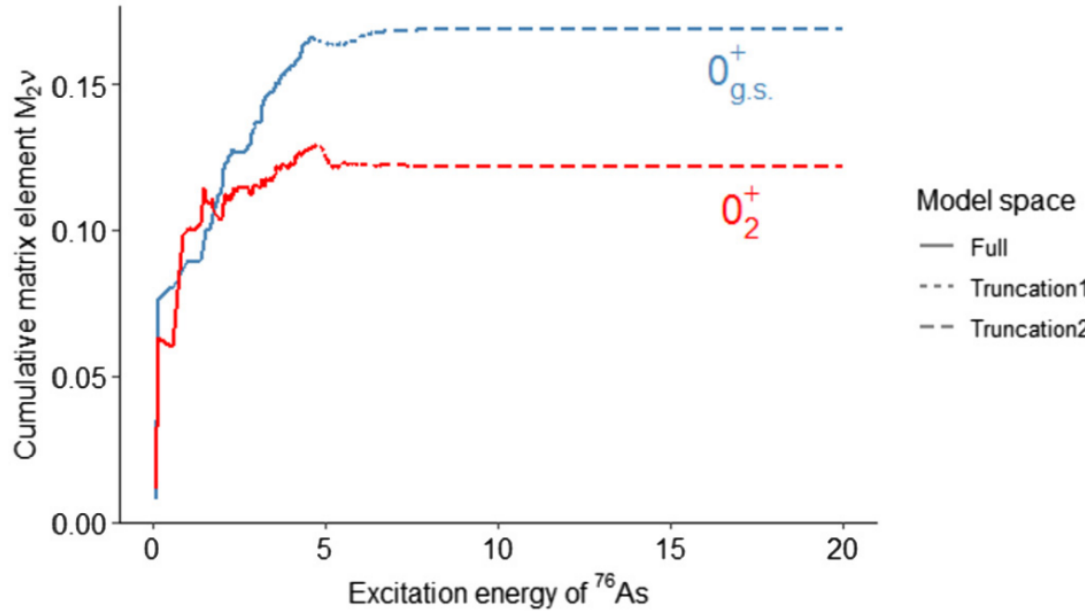


**Fig. 1.** Cumulative  $2\nu\beta\beta$  NMEs  $M_{2\nu}$  for the decay of  $^{76}\text{Ge}$  to the  $0_{\text{g.s.}}^+$  and  $0_2^+$  states in  $^{76}\text{Se}$  as functions of the excitation energy of the intermediate states in  $^{76}\text{As}$ . The full calculation (solid line) has been carried out in the  $0f_{5/2} - 1p - 0g_{9/2}$  model space, for truncation 1 (dotted line) the neutron orbital  $0g_{5/2}$  was kept full and for Truncation 2 (dashed line), additionally, the proton orbital  $0g_{9/2}$  was kept empty.

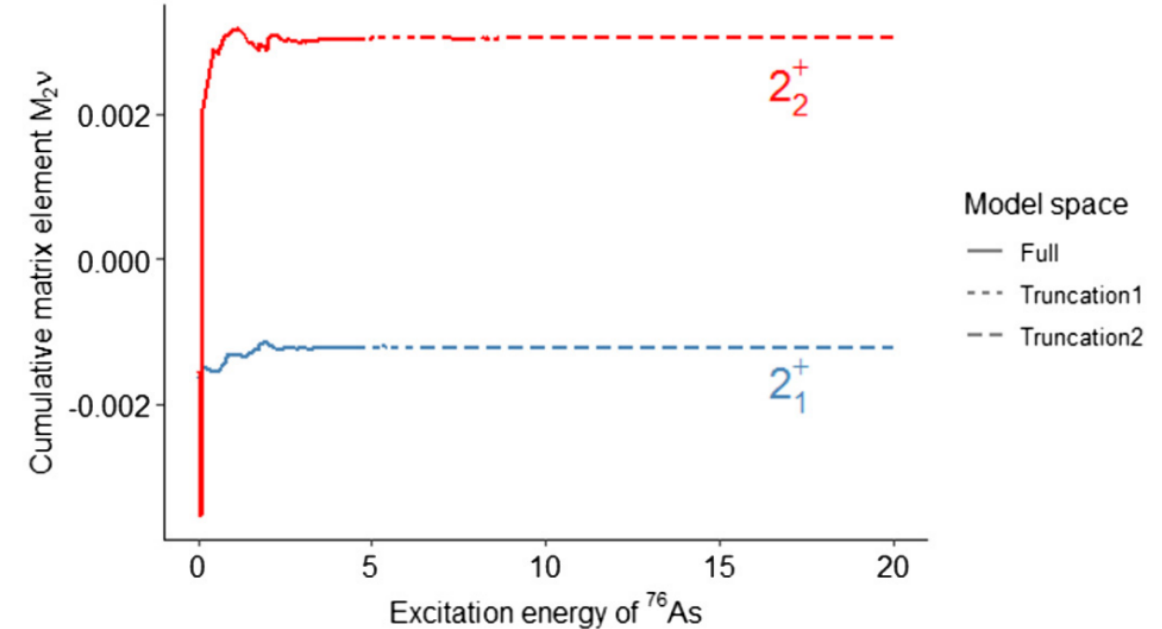


**Fig. 2.** The same as in Fig. 1 for cumulative  $2\nu\beta\beta$  NMEs  $M_{2\nu}$  of the decay of  $^{76}\text{Ge}$  to the  $2_1^+$  and  $2_2^+$  states in  $^{76}\text{Se}$ .

# COMPARISON WITH PREVIOUS THEORETICAL ESTIMATES

**Table 2**

Comparison of the presently computed  $2\nu\beta\beta$  NMEs (last line) with earlier calculations for the  $0_{g.s.}^+$ ,  $2_1^+$ ,  $0_2^+$  and  $2_2^+$  states (columns 1-4). Column 5 indicates the used theory, with MCM=Multiple Commutator Model, HQRPA=Higher QRPA, RQRPA=Renormalized QRPA, SM=shell model. The last column gives the reference to the calculation.

$ M_{2\nu}(0_{g.s.}^+) $	$ M_{2\nu}(2_1^+) $	$ M_{2\nu}(0_2^+) $	$ M_{2\nu}(2_2^+) $	Theory	Ref.
0.074	$1 \times 10^{-3}$	0.363	$3 \times 10^{-3}$	MCM	[13]
-	$2 \times 10^{-3}$	-	-	HQRPA	[15]
0.100	$3 \times 10^{-3}$	0.838	$3 \times 10^{-3}$	MCM	[14]
0.083	0.013	0.056	-	HQRPA	[16]
0.074	$3 \times 10^{-3}$	$0.130 - 0.229$	$(7 - 12) \times 10^{-3}$	RQRPA	[19]
-	$(0.48 - 0.65) \times 10^{-3}$	-	-	RQRPA	[20]
0.113	$0.74 \times 10^{-3}$	-	-	HRPA	[17]
0.168	$1.2 \times 10^{-3}$	0.121	$3.1 \times 10^{-3}$	SM	This work

# COMPARISON WITH THEORETICAL LOWER LIMITS FOR HALF-LIFE

**Table 1**

Shell-model calculated  $2\nu\beta\beta$  NMEs, phase-space integrals and half-lives (columns 3-5) for the decay of  $^{76}\text{Ge}$  to the ground state and lowest three excited states (column 1) of  $^{76}\text{Se}$ . The phase-space integrals for the lowest three states are taken from [21] and the fourth one has been calculated using the formulas of this reference. Experimental Q values (column 2) are used in the calculations. The half-life for the ground-state transition matches the measured one [9] and the rest of the half-lives are based on the shell model calculations using  $g_A = 0.80 \pm 0.01$ , derived from the comparison of the computed half-life with the experimental one for the ground-state transition. The uncertainties include only the uncertainty related to the value of the experimental half-life of the ground-state transition. In the sixth column we list the measured lower limits for the half-lives, including the corresponding reference in the last column.

$J_f^\pi$	$Q_{\beta\beta}$ (keV)	$ M_{2\nu} $	$G$ ( $\text{yr}^{-1}$ )	$T_{1/2}^{\beta\beta}(\text{th.})$ (yr)	$T_{1/2}^{\beta\beta}(\text{exp.})$ (yr)	Ref.
$0_{\text{gs}}^+$	2039	0.168	$4.51 \times 10^{-20}$	$(1.926 \pm 0.094) \times 10^{21}$	$(1.926 \pm 0.094) \times 10^{21}$	[9]
$2_1^+$	1480	$1.2 \times 10^{-3}$	$4.0 \times 10^{-22}$	$(4.37 \pm 0.20) \times 10^{27}$	$> 1.1 \times 10^{21}$	[32]
$0_2^+$	917	0.121	$6.4 \times 10^{-23}$	$(2.60 \pm 0.13) \times 10^{24}$	$> 6.2 \times 10^{21}$	[31]
$2_2^+$	823	$3.1 \times 10^{-3}$	$3.33 \times 10^{-25}$	$(7.57 \pm 0.37) \times 10^{29}$	$> 1.4 \times 10^{21}$	[32]

## Up-to-date limits:

$> 7.7 \times 10^{23}$  ( $2_1^+$ )

I. J. Arnquist et al. (MAJORANA Collaboration)  
Phys. Rev. C **103**, 015501 – Published 6 January 2021 (90%  
C.L.).

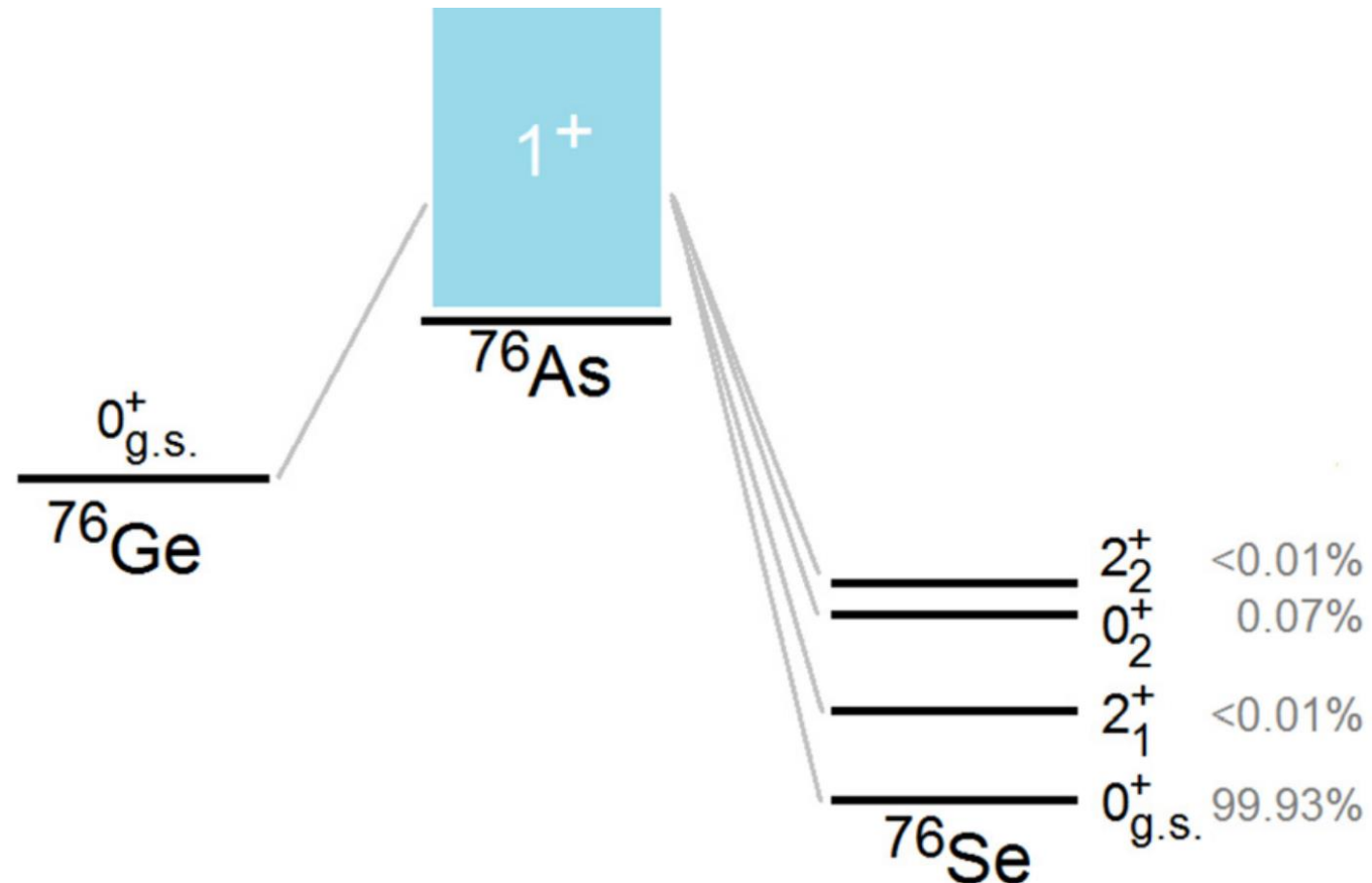
$> 7.5 \times 10^{23}$  ( $0_2^+$ )

$> 12.8 \times 10^{23}$  ( $2_2^+$ )

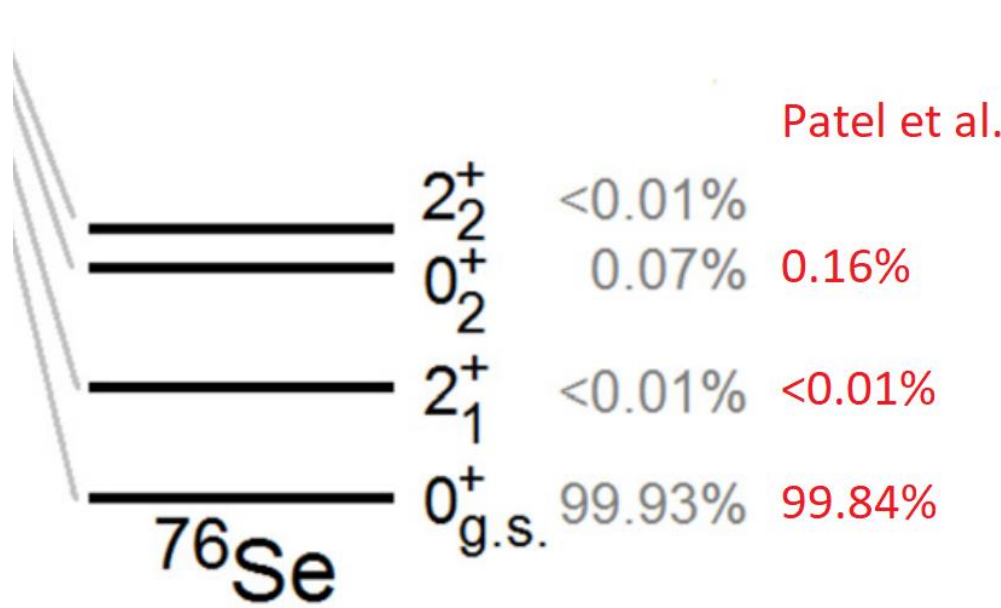
[31] A.A. Klimenko, et al., Czechoslov. J. Phys. 52 (2002) 589.

[32] A.S. Barabash, A.V. Derbin, L.A. Popeko, V.I. Umatov, Z. Phys. A 352 (1995) 231.

# PREDICTED BRANCHINGS



## RECENT DEVELOPMENTS (SINCE PUBLICATION)



- GERDA updated the gs-to-gs half-life (Oct. 2023) to  $(2.022 \pm 0.018_{\text{stat}} \pm 0.038_{\text{syst}}) \times 10^{21}$  yr from  $(1.926 \pm 0.095) \times 10^{21} \rightarrow 5\%$  longer, twice as accurate.
- Patel et al. (2024) [pre-print] carried out another large-scale shell-model calculation using the Hamiltonian GWBXG.
- The experimental half-life limit  $> 7.5 \times 10^{23}$  yr ( $0^+_2$ ) is getting close to the theoretical estimates  $1 - 3 \times 10^{24}$  yr.

# $^{48}\text{Ca}$ and $^{96}\text{Zr}$

## $2\nu\beta\beta$ vs. $\beta$ -decays

Kostensalo, J., & Suhonen, J. (2020). Consistent large-scale shell-model analysis of the two-neutrino  $\beta\beta$  and single  $\beta$  branchings in  $^{48}\text{Ca}$  and  $^{96}\text{Zr}$ . *Physics Letters B*, 802, Article 135192. <https://doi.org/10.1016/j.physletb.2019.135192>

# DOUBLE BETA AND BETA DECAYS

$$Q_{\beta\beta} = 4268 \text{ keV}$$

$$Q_\beta = 279/146/27 \text{ keV } (6+/5+/4+)$$

$$T_{1/2\beta\beta} = \sim 5.6 \times 10^{19} \text{ yr}$$

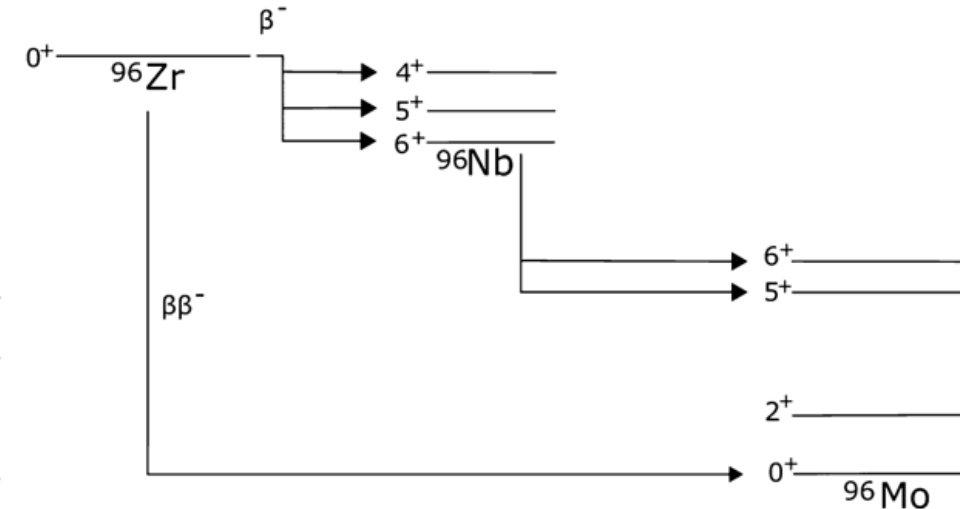
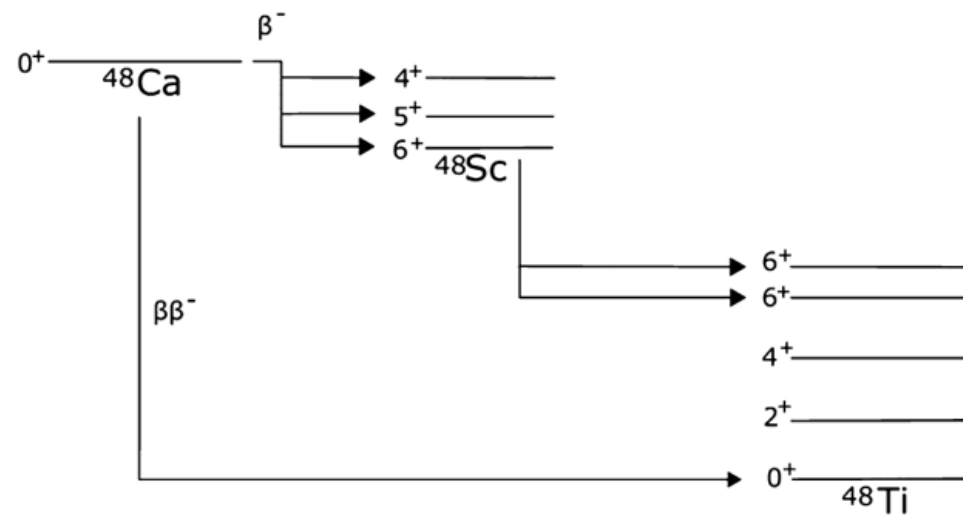
$$T_{1/2\beta} = ???$$

$$Q_{\beta\beta} = 3356 \text{ keV}$$

$$Q_\beta = 164/120/18 \text{ keV } (6+/5+/4+)$$

$$T_{1/2\beta\beta} = \sim 2.3 \times 10^{19} \text{ yr}$$

$$T_{1/2\beta} = ???$$



## SINGLE BETA DECAYS: LIMITS

Best experimental limits for single beta decays according to Tretyak, AIP Conf. Proc. 1894, 020026 (2017):

$^{48}\text{Ca}$ :  $>2.5 \times 10^{20}$  yr A. Bakalyarov et al., JETP Lett. 76, 545 (2002).

$^{96}\text{Zr}$ :  $>3.8 \times 10^{19}$  yr M. Arpesella et al., Europhys. Lett. 27, 29 (1994).

# DESCRIPTION OF THE SHELL-MODEL CALCULATIONS

- $^{48}\text{Ca}$ : calculation in the full  $fp$  model space with *GFPXIA*. Effective  $g_A$  fixed by two-beta decay half-life (same value used for single and double beta decay). 9470 intermediate  $I^+$  states (60 MeV).
- $^{96}\text{Zr}$ : Full model space with proton orbitals  $0f_{5/2}-1p-0g_{9/2}$  and neutron orbitals  $0g_{7/2}-1d-2s_{1/2}$  with *glekpn*. 5894 intermediate  $I^+$  states (18 MeV).

# CUMULATIVE NME

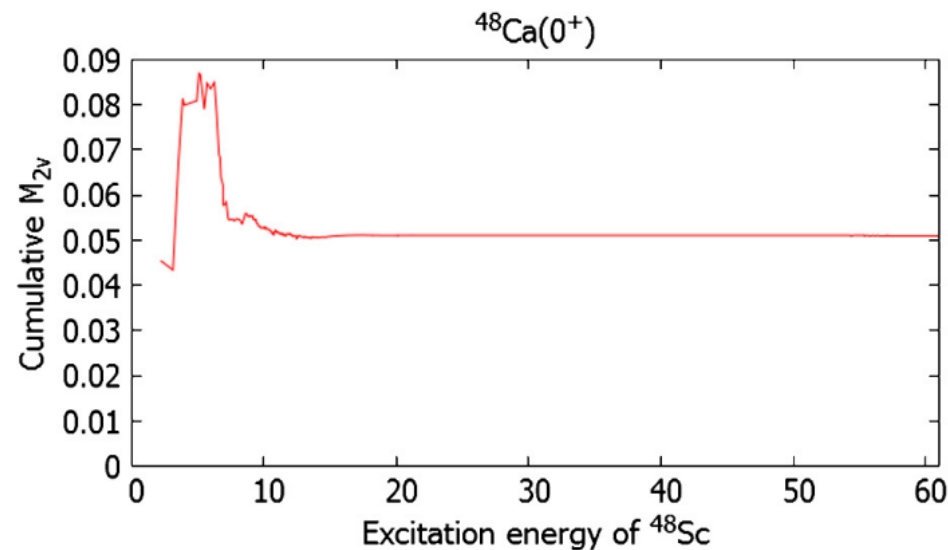


**Fig. 1.** Cumulative  $2\nu\beta\beta$  NME  $M_{2v}$  for  $^{48}\text{Ca}$  as a function of excitation energy of the intermediate state in  $^{48}\text{Sc}$ .

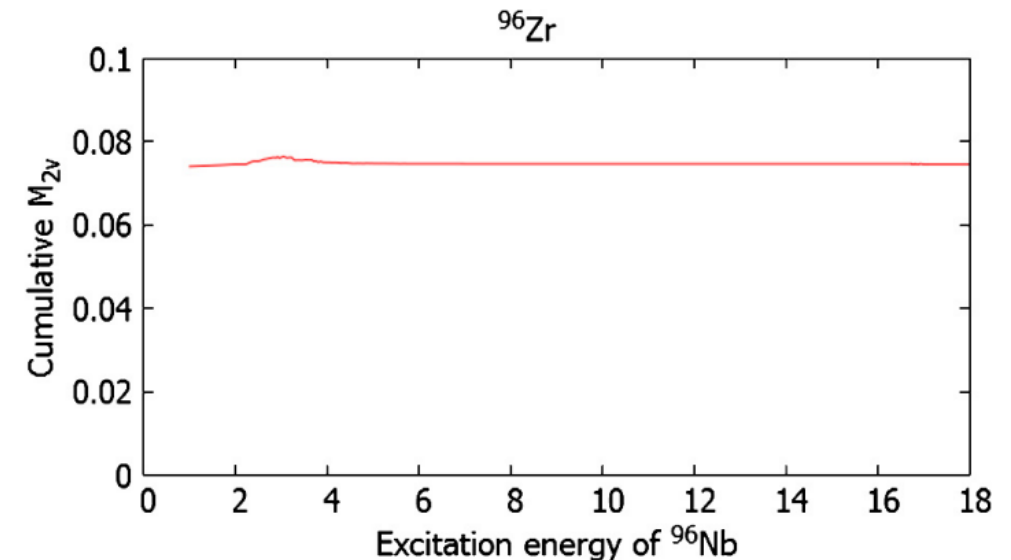


**Fig. 2.** Cumulative  $2\nu\beta\beta$  NME  $M_{2v}$  for  $^{96}\text{Zr}$  as a function of excitation energy of the intermediate state in  $^{96}\text{Nb}$ .

# BRANCHING RATIO AND AXIAL-VECTOR COUPLING

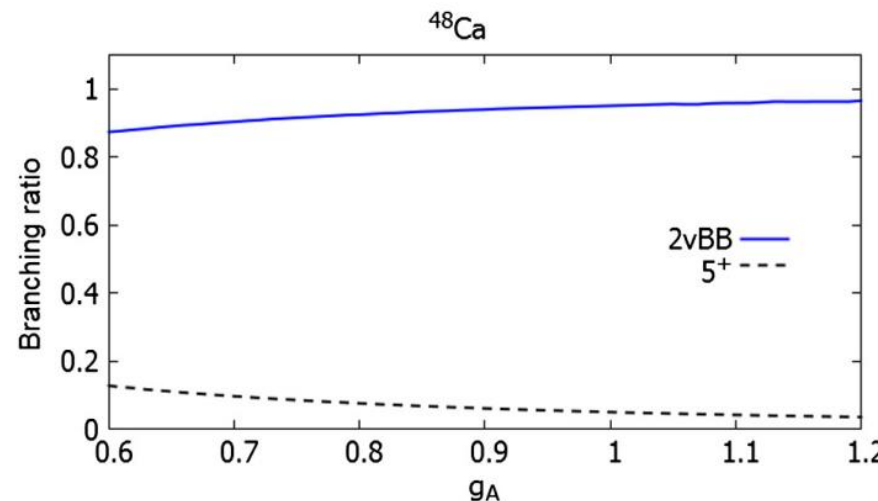


**Fig. 5.** Branching ratios of the two dominant branches of  $^{48}\text{Ca}$  as functions of  $g_A$ .

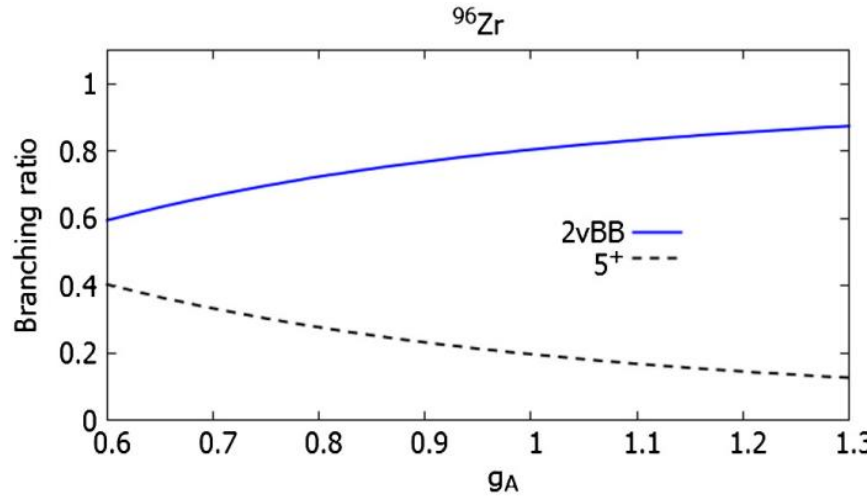


**Fig. 8.** Branching ratios of the two dominant branches of  $^{96}\text{Zr}$  as functions of  $g_A$ .

**Table 1**

Shell-model calculated  $2\nu\beta\beta$  NMEs and the extracted effective value  $g_A^{\text{eff}}$  of the axial-vector coupling.

Nucleus	$ M_{2\nu} $	$G (10^{-18} \text{ yr}^{-1})$ [25]	$T_{1/2}^{\beta\beta} (10^{19} \text{ yr})$	$g_A^{\text{eff}}$
$^{48}\text{Ca}$	0.0511	14.805	$6.4^{+1.4}_{-1.1}$ [9]	$0.80 \pm 0.04$
$^{96}\text{Zr}$	0.0747	6.420	$2.35 \pm 0.21$ [10]	$1.04^{+0.03}_{-0.02}$

[9] R. Arnold, C. Augier, A.M. Bakalyarov, J.D. Baker, A.S. Barabash, et al., NEMO-3 Collaboration, Phys. Rev. D 93 (2016) 112008.

[10] J. Argyriades, R. Arnold, C. Augier, J. Baker, A. Barabash, et al., Nucl. Phys. A 847 (2010) 168.

# PREDICTED BRANCHING RATIOS

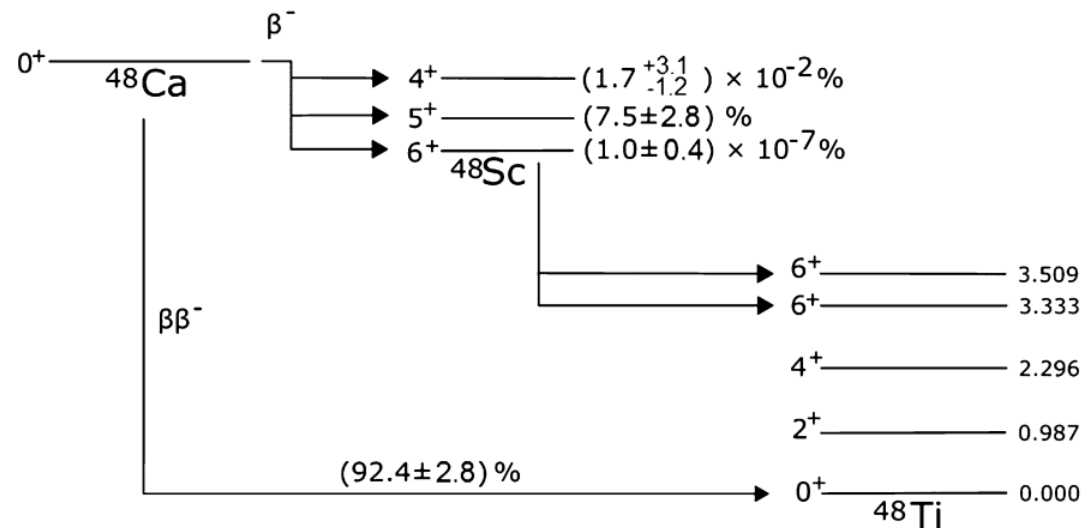


**Fig. 3.** Decay scheme of  $^{48}\text{Ca}$ . Also indicated are our shell-model computed  $\beta$ -decay and  $2\nu\beta\beta$ -decay branching ratios.

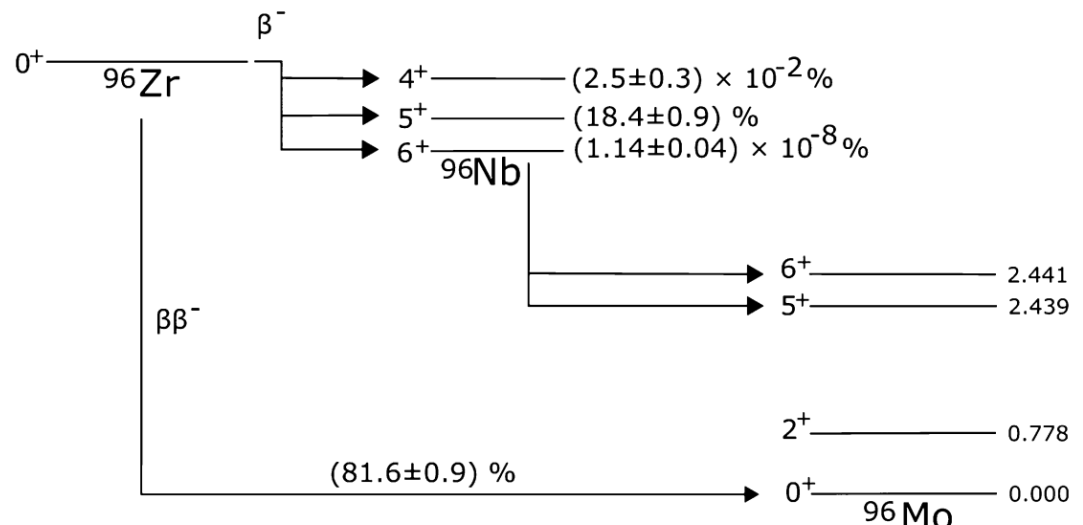


**Fig. 6.** Decay scheme of  $^{96}\text{Zr}$ . Also indicated are our shell-model computed  $\beta$ -decay and  $2\nu\beta\beta$ -decay branching ratios.

# HOW CLOSE ARE THE EXPERIMENTAL LIMITS?

$^{48}\text{Ca}$ :

$\sim 8 \times 10^{20} \text{ yr}$  (**shell model**)

$\sim 3.4 \times 10^{20} \text{ yr}$  (*shell model, Haaranen et al., 2014*)

$> 2.5 \times 10^{20} \text{ yr}$  \* (*exp. limit*)

$^{96}\text{Zr}$ :

$\sim 1 \times 10^{20} \text{ yr}$  (**shell model**)

$\sim 2.4 \times 10^{20} \text{ yr}$  (*p<sub>n</sub>QRPA – Heiskanen et al., 2007*)

$> 3.8 \times 10^{19} \text{ yr}$  \*\* (*exp. limit*)

**Table 1**

Shell-model calculated  $2\nu\beta\beta$  NMEs and the extracted effective value  $g_A^{\text{eff}}$  of the axial-vector coupling.

Nucleus	$ M_{2\nu} $	$G (10^{-18} \text{ yr}^{-1})$ [25]	$T_{1/2}^{\beta\beta} (10^{19} \text{ yr})$	$g_A^{\text{eff}}$
$^{48}\text{Ca}$	0.0511	14.805	$6.4_{-1.1}^{+1.4}$ [9]	$0.80 \pm 0.04$
$^{96}\text{Zr}$	0.0747	6.420	$2.35 \pm 0.21$ [10]	$1.04_{-0.02}^{+0.03}$

[9] R. Arnold, C. Augier, A.M. Bakalyarov, J.D. Baker, A.S. Barabash, et al., NEMO-3 Collaboration, Phys. Rev. D 93 (2016) 112008.

[10] J. Argyriades, R. Arnold, C. Augier, J. Baker, A. Barabash, et al., Nucl. Phys. A 847 (2010) 168.

\* A. Bakalyarov et al., JETP Lett. 76, 545 (2002).

\*\* M. Arpesella et al., Europhys. Lett. 27, 29 (1994).

# $^{71}\text{Ga}$

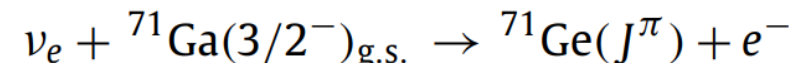
## Evidence for sterile neutrinos?

Kostensalo, J., Suhonen, J., Giunti, C., & Srivastava, P. C. (2019). The gallium anomaly revisited. *Physics Letters B*, 795, 542-547. <https://doi.org/10.1016/j.physletb.2019.06.057>

Corrigendum to “The gallium anomaly revisited” [Phys. Lett. B 795 (2019) 542–547]  
*Physics Letters B*, 846, 138190 (2023).

# THE GALLIUM ANOMALY

- GALLEX and SAGE experiments were designed to detect neutrinos utilizing the transition



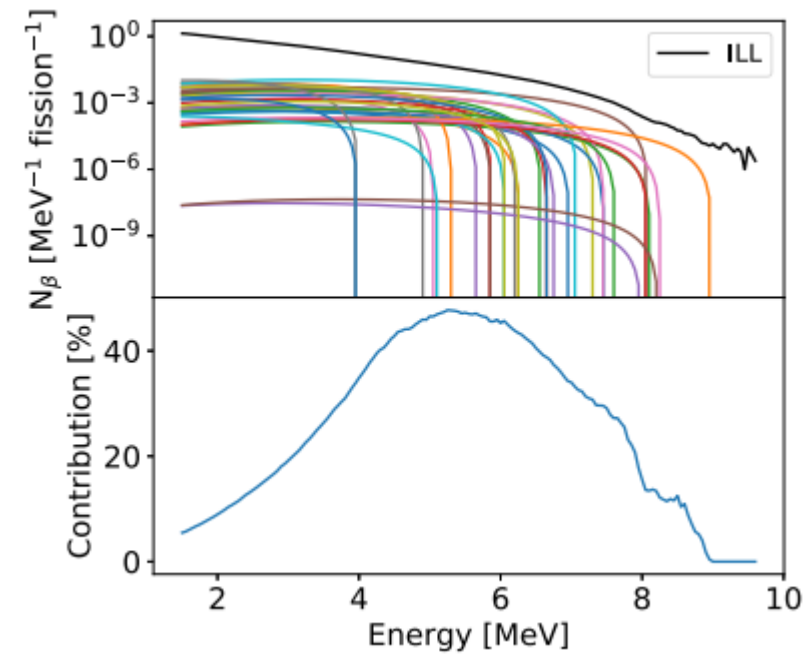
- Source experiments with  ${}^{51}\text{Cr}$  and  ${}^{37}\text{Ar}$  neutrinos showed slightly lower fluxes than predicted by Bahcall based on (p,n)-reaction cross sections.
- Haxton (1998) showed that charge-exchange reactions may be unreliable in this case due to tensor contributions because the transition to the  $5/2^-$  state is *L-forbidden*.
- Missing neutrino flux could potentially be an indication of *sterile neutrinos*.
- Reactor antineutrino anomaly could potentially also be explained by sterile neutrinos.

# EXCURSION: REACTOR ANTINEUTRINO ANOMALY

Hayen, L., Kostensalo, J.,  
Severijns, N., & Suhonen, J.  
(2019). First-forbidden  
transitions in the reactor  
anomaly. *Physical Review C*, 100(5), Article  
054323. <https://doi.org/10.1103/PhysRevC.100.054323>

- Missing neutrino flux from reactors (~5%)
- Spectral shoulder (“bump”) at ~5 MeV
- Previous theoretical calculations missing forbidden transitions

Nuclide	$Q_\beta$ (MeV)	$E_{\text{ex}}$ (MeV)	BR (%)	$J_i^\pi \rightarrow J_f^\pi$	FY (%)	$\Delta J$
<sup>89</sup> Br	8.3	0	16	$3/2^- \rightarrow 3/2^+$	1.1	0
<sup>90</sup> Rb	6.6	0	33	$0^- \rightarrow 0^+$	4.5	0
<sup>91</sup> Kr	6.8	0.11	18	$5/2^+ \rightarrow 5/2^-$	3.5	0
<sup>92</sup> Rb	8.1	0	95.2	$0^- \rightarrow 0^+$	4.8	0
<sup>93</sup> Rb	7.5	0	35	$5/2^- \rightarrow 5/2^+$	3.5	0
<sup>94</sup> Y	4.9	0.92	39.6	$2^- \rightarrow 2^+$	6.5	0
<sup>95</sup> Rb <sup>a</sup>	9.3	0.68	5.9	$5/2^- \rightarrow 5/2^+$	1.7	0
<sup>95</sup> Sr	6.1	0	56	$1/2^+ \rightarrow 1/2^-$	5.3	0
<sup>96</sup> Y	7.1	0	95.5	$0^- \rightarrow 0^+$	6.0	0
<sup>97</sup> Y	6.8	0	40	$1/2^- \rightarrow 1/2^+$	4.9	0
<sup>98</sup> Y	9.0	0	18	$0^- \rightarrow 0^+$	1.9	0
<sup>133</sup> Sn	8.0	0	85	$7/2^- \rightarrow 7/2^+$	0.1	0
<sup>135</sup> Te	5.9	0	62	$(7/2-) \rightarrow 7/2^+$	3.3	0
<sup>135</sup> Sb	8.1	0	47	$(7/2+) \rightarrow (7/2^-)$	0.1	0
<sup>136m</sup> I	7.5	1.89	71	$(6^-) \rightarrow 6^+$	1.3	0
<sup>136m</sup> I	7.5	2.26	13.4	$(6^-) \rightarrow 6^+$	1.3	0
<sup>137</sup> I	6.0	0	45.2	$7/2^+ \rightarrow 7/2^-$	3.1	0
<sup>142</sup> Cs	7.3	0	56	$0^- \rightarrow 0^+$	2.7	0
<sup>86</sup> Br	7.3	0	15	$(1^-) \rightarrow 0^+$	1.6	1
<sup>86</sup> Br	7.3	1.6	13	$(1^-) \rightarrow 2^+$	1.6	1
<sup>87</sup> Se	7.5	0	32	$3/2^+ \rightarrow 5/2^-$	0.8	1
<sup>89</sup> Br	8.3	0.03	16	$3/2^- \rightarrow 5/2^+$	1.1	1
<sup>91</sup> Kr	6.8	0	9	$5/2^+ \rightarrow 3/2^-$	3.4	1
<sup>95</sup> Rb <sup>a</sup>	9.3	0.56	6.0	$5/2^- \rightarrow (7/2^+)$	1.7	1
<sup>95</sup> Rb	9.3	0.68	5.9	$5/2^- \rightarrow 3/2^+$	1.7	1
<sup>134m</sup> Sb	8.5	1.69	42	$(7-) \rightarrow 6^+$	0.8	1
<sup>134m</sup> Sb	8.5	2.40	54	$(7-) \rightarrow (6^+)$	0.8	1
<sup>136</sup> Te	5.1	0	8.7	$0^+ \rightarrow (1^-)$	3.7	1
<sup>138</sup> I	8.0	0	26	$(1-) \rightarrow 0^+$	1.5	1
<sup>140</sup> Xe	4.0	0.08	8.7	$0^+ \rightarrow 1^-$	4.9	1
<sup>140</sup> Xe	6.2	0	36	$1^- \rightarrow 0^+$	5.7	1
<sup>143</sup> Cs	6.3	0	25	$3/2^+ \rightarrow 5/2^-$	1.5	1
<sup>88</sup> Rb	5.3	0	76.5	$2^- \rightarrow 0^+$	3.6	2
<sup>94</sup> Y	4.9	0	41	$2^- \rightarrow 0^+$	6.5	2
<sup>95</sup> Rb	9.3	0	0.1	$5/2^- \rightarrow 1/2^+$	1.7	2
<sup>139</sup> Xe	5.1	0	15	$3/2^- \rightarrow 7/2^+$	5.0	2



# EXCURSION: REACTOR ANTINEUTRINO ANOMALY

HAYEN, L., KOSTENSALO, J.,  
SEVERIJNS, N., & SUHONEN, J.  
(2019). FIRST-FORBIDDEN  
TRANSITIONS IN THE REACTOR  
ANOMALY. *PHYSICAL REVIEW C*, 100(5), ARTICLE  
054323. [HTTPS://DOI.ORG/10.1103/PHYSREVC.100.054323](https://doi.org/10.1103/PHYSREVC.100.054323)

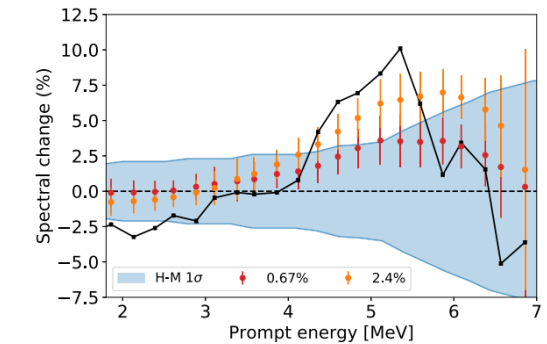
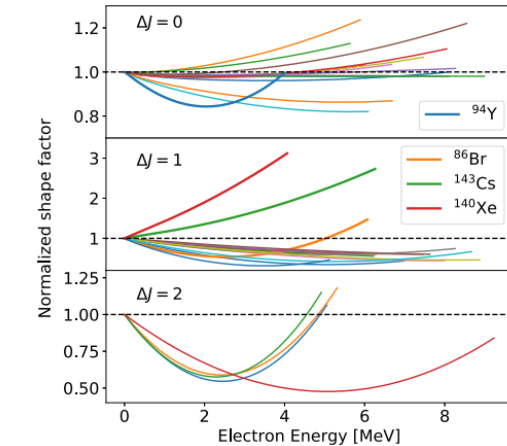


FIG. 18. Comparison of the Daya Bay shape discrepancy with the change due to the forbidden shape factors of Sec. IV when compared to two different slopes of the allowed approximation: 0.67% and 2.4%, as discussed in Secs. II D and VII B 1.

- Some flux still missing
- Spectral shoulder mitigated
- Uncertainties increase significantly

# DESCRIPTION OF THE SHELL-MODEL CALCULATIONS

- Calculation in the full  $0f_{5/2}$ - $1p$ - $0g_{9/2}$  model space without truncations.
- Effective interaction JUN45.
- Good agreement with known electric and magnetic moments.

# ENERGY SPECTRA

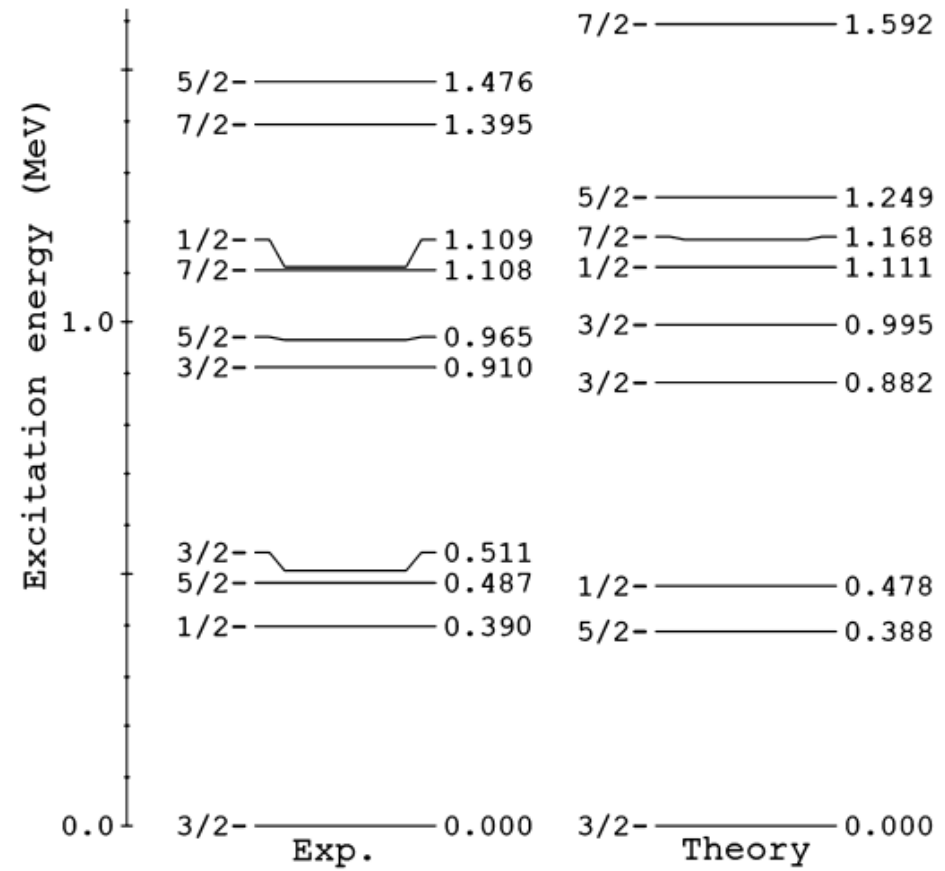


Fig. 1. Experimental and theoretical low-lying energy spectra of  $^{71}\text{Ga}$ .

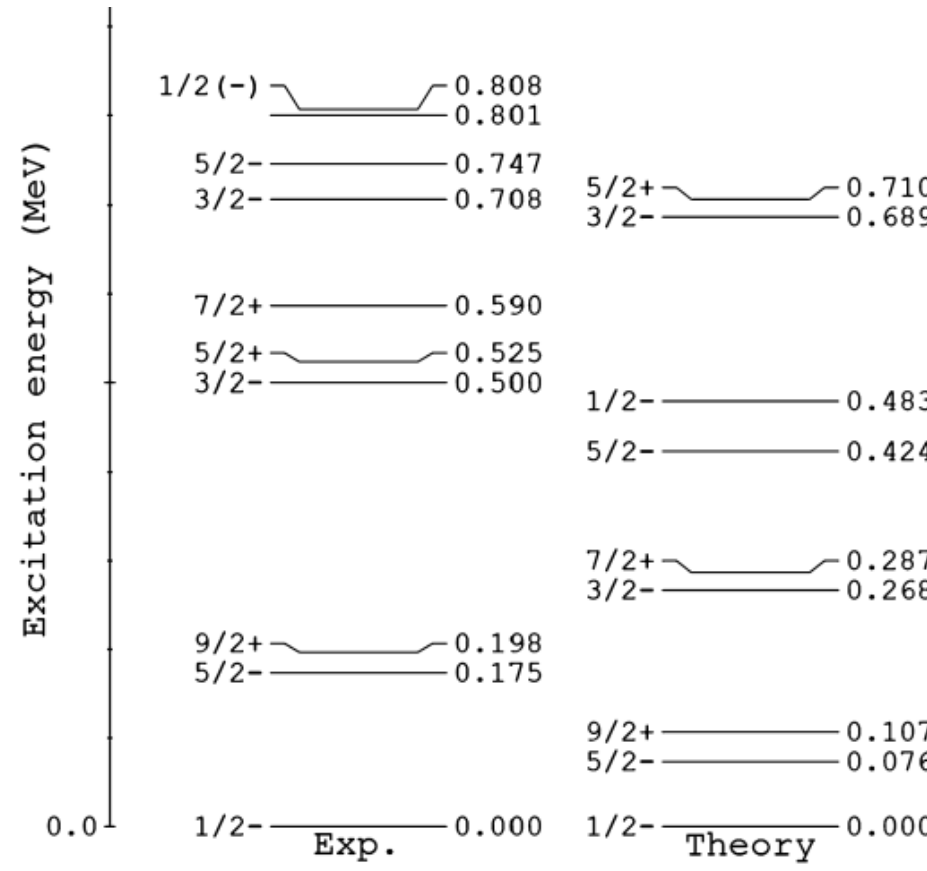


Fig. 2. Experimental and theoretical low-lying energy spectra of  $^{71}\text{Ge}$ .

# HOW TO EVALUATE THE CROSS SECTION?

$$\sigma = \sigma_{\text{gs}} \left( 1 + \xi_{5/2-} \frac{\text{BGT}_{5/2-}}{\text{BGT}_{\text{gs}}} + \xi_{3/2-} \frac{\text{BGT}_{3/2-}}{\text{BGT}_{\text{gs}}} \right)$$

$$\xi_{5/2-}(^{51}\text{Cr}) = 0.663$$

$$\xi_{3/2-}(^{51}\text{Cr}) = 0.221$$

$$\xi_{5/2-}(^{37}\text{Ar}) = 0.691$$

$$\xi_{3/2-}(^{37}\text{Ar}) = 0.262$$

$$\sigma_{\text{gs}}(^{51}\text{Cr}) = (5.53 \pm 0.01) \times 10^{-45} \text{ cm}^2,$$

$$\sigma_{\text{gs}}(^{37}\text{Ar}) = (6.62 \pm 0.01) \times 10^{-45} \text{ cm}^2.$$

- GS-cross sections from half-life of  ${}^{71}\text{Ge}$ .
- Phase-space factors from kinematics.
- BGT-ratios are non-trivial:
  - Charge-exchange reaction
  - Theoretical calculation

# CROSS SECTIONS FROM CHARGE EXCHANGE REACTIONS

- Haxton (1998): Cross sections based on charge-exchange reactions can be described well with the effective operator:

$$\langle f || O_{(p,n)} || i \rangle = \langle f || O_{\text{GT}} || i \rangle + \delta \langle f || O_{L=2} || i \rangle$$

- Based on (p,n)-reaction data, the mixing parameter  $\delta$  is about  $\sim 0.1$ .
- The transition to  $5/2^-$  would be predominantly between the orbitals  $0f5/2$  and  $1p3/2 \rightarrow$  single-particle GT identically zero, i.e.,  $L$ -forbidden! Tensor contribution becomes important.
- Kostensalo et al. (2019): BGT for ground state underestimated, BGT for  $3/2^-$  overestimated  $\rightarrow$  systematic overestimation.

# SYSTEMATIC PROBLEMS WITH CHARGE-EXCHANGE CROSS SECTIONS

Table 1. Results for  $^{71}\text{Ga}$  with  $\delta=0.097$  and corrected tensor matrix elements.

State	$\langle f    \mathcal{O}_{GT}    i \rangle$	$\langle f    \mathcal{O}_{L=2}    i \rangle$	$BGT_{\beta}^{\text{SM}}$	$BGT_{(p,n)}^{\text{SM}}$	
$1/2_{g.s.}^-$	-0.795	0.521	0.158	0.139	Underestimation
$5/2_1^-$	0.144	-0.763	0.0052	0.0012	Extremely sensitive
$3/2_1^-$	0.100	0.0687	0.0025	0.0028	Overestimation

# CONTRIBUTIONS FOR THE EXCITED STATES ARE LOWER

**Table 6**

Values of the Gamow-Teller strengths of the transitions from the ground state of  $^{71}\text{Ga}$  to the relevant excited states of  $^{71}\text{Ge}$  relative to the Gamow-Teller strength of the transitions to the ground state of  $^{71}\text{Ge}$  obtained by Krofcheck et al. [36,37], Haxton [8], Frekers et al. [5], and with the JUN45 calculation presented in this paper.

	Method	$\frac{\text{BGT}_{5/2-}}{\text{BGT}_{\text{gs}}}$	$\frac{\text{BGT}_{3/2-}}{\text{BGT}_{\text{gs}}}$	$\frac{\text{BGT}_{5/2+}}{\text{BGT}_{\text{gs}}}$
Krofcheck	$^{71}\text{Ga}(p, n)^{71}\text{Ge}$	$< 0.057$	$0.126 \pm 0.023$	
Haxton	Shell Model	$0.19 \pm 0.18$		
Frekers	$^{71}\text{Ga}({}^3\text{He}, {}^3\text{H})^{71}\text{Ge}$	$0.040 \pm 0.031$	$0.207 \pm 0.016$	
JUN45	Shell Model	$(3.30 \pm 1.66) \times 10^{-2}$	$(1.59 \pm 0.79) \times 10^{-2}$	$(4.46 \pm 2.24) \times 10^{-6}$

# GALLIUM ANOMALY IS SMALLER, BUT DOES NOT DISAPPEAR

**Table 7**

Ratios of measured and expected  ${}^{71}\text{Ge}$  event rates in the four radioactive source experiments, their correlated average, and the statistical significance of the gallium anomaly obtained with the cross sections in Table 5.

	GALLEX-1	GALLEX-2	SAGE-1	SAGE-2	Average	Anomaly
$R_{\text{Bahcall}}$	$0.95 \pm 0.11$	$0.81 \pm 0.11$	$0.95 \pm 0.12$	$0.79 \pm 0.08$	$0.85 \pm 0.06$	$2.6\sigma$
$R_{\text{Haxton}}$	$0.86 \pm 0.13$	$0.74 \pm 0.12$	$0.86 \pm 0.14$	$0.72 \pm 0.10$	$0.76 \pm 0.10$	$2.5\sigma$
$R_{\text{Frekers}}$	$0.93 \pm 0.11$	$0.79 \pm 0.11$	$0.93 \pm 0.12$	$0.77 \pm 0.08$	$0.84 \pm 0.05$	$3.0\sigma$
$R_{\text{JUN45}}$	$0.97 \pm 0.11$	$0.83 \pm 0.11$	$0.97 \pm 0.12$	$0.81 \pm 0.08$	$0.88 \pm 0.05$	$2.3\sigma$

# AGREEMENT WITH REACTOR DATA IS SIGNIFICANTLY IMPROVED

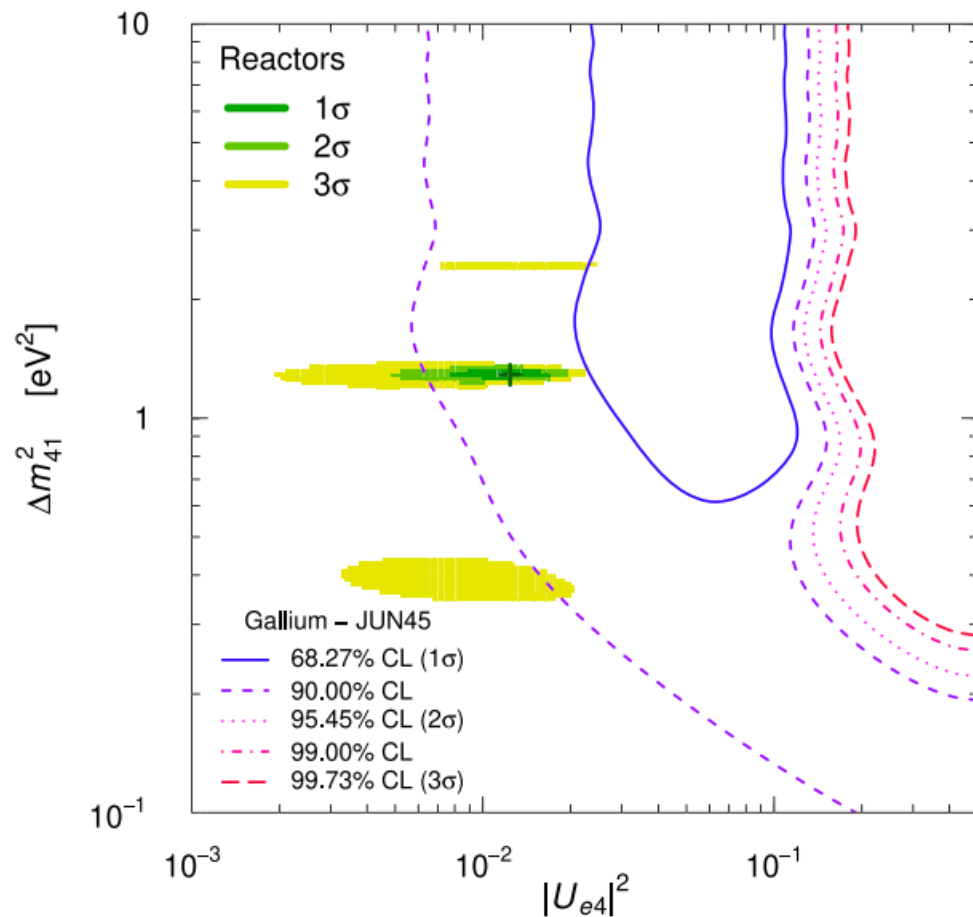


Fig. 4 shows the comparison of the allowed regions in the  $|U_{e4}|^2 - \Delta m_{41}^2$  plane obtained with our JUN45 shell model for different confidence levels with the regions obtained from the combined analysis of the data of the NEOS and DANSS reactor experiments, to which we have added the more recent data of the PROSPECT [48] reactor experiment that excludes large values of  $|U_{e4}|^2$  for  $0.7 \lesssim \Delta m_{41}^2 \lesssim 7$  eV<sup>2</sup>. One can see that there is an overlap of the 90% CL allowed regions, indicating a reasonable agreement between the gallium anomaly and the reactor data. The corresponding parameter goodness of fit is a favorable 16% ( $\Delta\chi^2/NDF = 3.6/2$ ).

**Fig. 4.** Comparison of the allowed regions in the  $|U_{e4}|^2 - \Delta m_{41}^2$  plane obtained from the Gallium data with the JUN45 cross sections and the allowed regions obtained from the analysis of the data of the NEOS, DANSS and PROSPECT reactor experiments.

# SUMMARY

- Experimental limits of three transitions are closing in on theoretical half-lives.
- Good test cases for nuclear models.
- Shell-model calculations can give insights regarding charge-exchange reactions.
- Conflict between reactor antineutrino anomaly and the gallium anomaly is mitigated by the new calculations.

# SUMMARY

**Decays soon to be discovered:**

**$^{76}\text{Ge}$ :**

$\sim 2.6 \times 10^{24} \text{ yr}$  (shell model)

$>7.5 \times 10^{23} \text{ yr}$  \*\* (exp. limit)

**$^{48}\text{Ca}$ :**

$\sim 8 \times 10^{20} \text{ yr}$  (shell model)

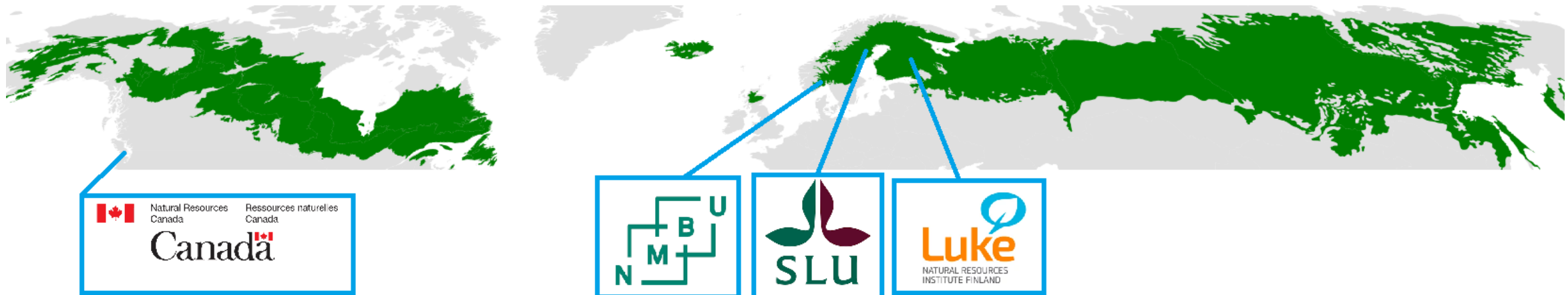
$>2.5 \times 10^{20} \text{ yr}$  \* (exp. limit)

**$^{96}\text{Zr}$ :**

$\sim 1 \times 10^{20} \text{ yr}$  (shell model)

$>3.8 \times 10^{19} \text{ yr}$  \*\* (exp. limit)

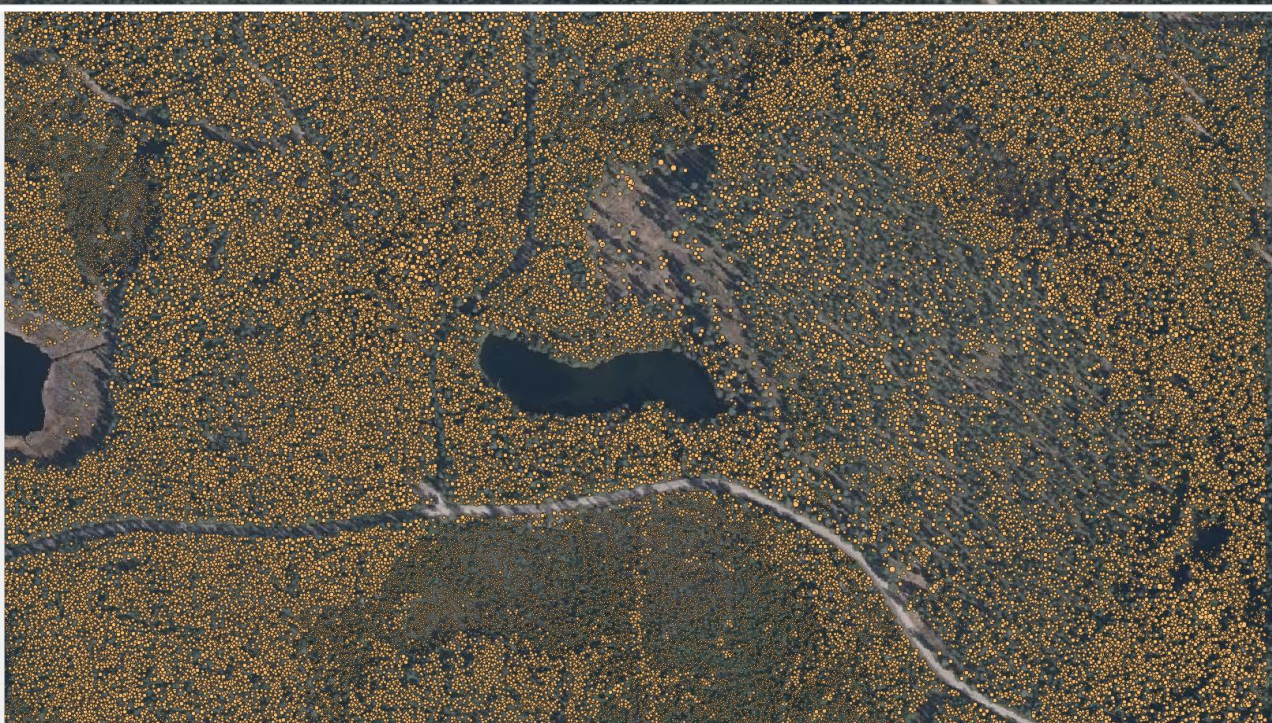
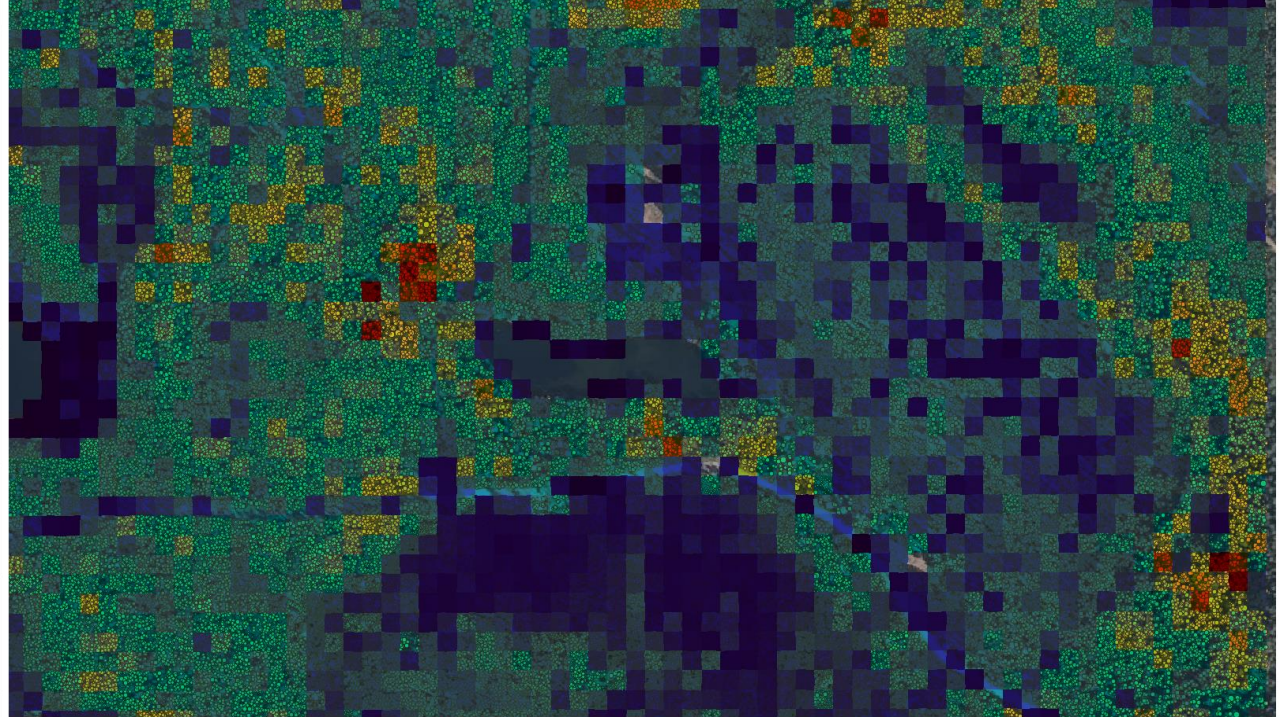
# WHAT AM I WORKING ON CURRENTLY?



## DigiTForest-project

- Four year project to create a digital twin of Boreal zone biodiversity
- > 1 000 000 € budget
- 2 postdoc positions







Research article

## A site-specific prediction model for nitrogen leaching in conventional and organic farming

Joel Kostensalo<sup>a</sup> , Riitta Lemola<sup>b</sup>, Tapio Salo<sup>b</sup>, Liisa Ukonmaanaho<sup>c</sup>, Eila Turtola<sup>b</sup>,  
Mattijs Soinne<sup>d</sup>



Research article

## Methodological choices in size and density fractionation of soil carbon reserves – A case study on wood fiber sludge amended soils

Riikka Keskinen<sup>a,\*</sup>, Johanna Nikama<sup>a</sup>, Joel Kostensalo<sup>b</sup>, Mari Räty<sup>c</sup>, Kimmo Rasa<sup>a</sup>,  
Helena Soinne<sup>d</sup>

<sup>a</sup> Natural Resources Institute Finland (LUKE), Tietotie 4, FI-31600, Jokioinen, Finland

<sup>b</sup> Natural Resources Institute Finland (LUKE), Yliopistonkatu 6 B, FI-80100, Joensuu, Finland

<sup>c</sup> Natural Resources Institute Finland (LUKE), Halokantie 31 A, FI-71750, Mäntsälä, Finland

<sup>d</sup> Natural Resources Institute Finland (LUKE), Latokarjankatu 9, FI-00790 Helsinki, Finland



## A Comprehensive Approach to PROMs in Elective Orthopedic Surgery: Comparing Effect Sizes across Patient Subgroups

by Ville Äärimaa<sup>1,2</sup> , Karita Kohtala<sup>2</sup> , Ida Rantalaaho<sup>1</sup> , Elina Ekman<sup>1</sup> , Keijo Mäkelä<sup>1,2</sup> , Hanna-Stiina Taskinen<sup>1</sup> , Anssi Ryösä<sup>1,2</sup> , Joel Kostensalo<sup>3</sup> , Saara Meronen<sup>1</sup> and Inari Laaksonen<sup>1,2</sup>

### Article Menu



## Temporal trends in Finnish agricultural soils: A comparative analysis of national and LUCAS soil monitoring datasets

Iaakko Heikkilä , Joel Kostensalo, Riikka Keskinen, Helena Soinne, Visa Nuutinen  
Received: Article

## Direct high-precision measurement of the mass difference of $^{77}\text{As}$ – $^{77}\text{Se}$ related to neutrino mass determination

Regular Article - Experimental Physics | Open access | Published: 08 May 2024

Volume 60, article number 104 (2024) | [Cite this article](#)

## Diversification of crop rotations and soil carbon balance: impact assessment based on national-scale monitoring data

Joel Kostensalo , Jari Hyväloma , Lauri Jauhainen , Riikka Keskinen , Visa Nuutinen , Pirjo Peltonen-Sainio & ...show all

Article: 2298373 | Received 16 May 2023, Accepted 17 Dec 2023, Published online: 07 Jan 2024

THANK YOU!

